ZANCO Journal of Pure and Applied Sciences
The official scientific journal of Salahaddin University-Erbil
https://zancojournals.su.edu.krd/index.php/JPAS

ISSN (print):2218-0230**, ISSN (online):** 2412-3986**, DOI: http://dx.doi.org/10.21271/zjpas**

RESEARCH PAPER

Intelligent System for Screening Diabetic Retinopathy by Using Neutrosophic and Statistical Fundus Image Features.

Bazhdar N. SH. Mohammed[1], Raghad Z. Yousif [1]

[1]Department of Physics, College of Science, Salahaddin University-Erbil, Kurdistan Region, Iraq

A B S T R A C T:

Diabetic retinopathy (DR) is considered as one of the global diseases of blindness, especially for aged people. The main reason behind this disease is the complication of diabetes in retinal blood vessels. Usually, the early warning signs are not observed. Screening is an important key for the diagnosis of early stages of diabetic retinopathy. In this work, a new technique for automatically screening three categories; Normal, Non-Proliferative Diabetic Retinopathy (Non-PDR), and Proliferative Diabetic Retinopathy (PDR) disease is presented that is may help doctors and physicians to make a preliminary decision. Neutrosophic set (NS) domain based on statistical features, Gray Level Cooccurrence Matrix (GLCM), Gray Level Run Length Matrix (GLRLM), and difference statistics were used for features extraction. More than thirty statistical textural features derived from the NS set domain and spatial domain have been tested using a features selection scheme named one-way analysis of variables (ANOVA1) with significance value ($p<0.001$). After feature selection, about sixteen features were passed the test and introduced to the classification stage which is made up of three techniques Multi-class support vector machine (MUSVM), Naïve Bayes (NB), and Decision Forest (DF) classifiers. Over 50 images from each category were downloaded from Digital Retinal Images for Vessel Extraction (DRIVE) database. The performance resulted for this proposed method shows the system robustness in identifying each stage of diabetic retinopathy within the accuracy, sensitivity, and specificity about 95.5%, 100%, and 93.3% respectively. The results of this method were compared with other considered systems. The fair comparison of results shows system superiority and can be used in clinical observation.

KEY WORDS: : Diabetic Retinopathy, Neutrosophic domain, Statistical features, Classification.
DOI: http://dx.doi.org/10.21271/ZJPAS.31.6.4
ZJPAS (2019), 31(6);30-39.

INTRODUCTION:

Automatic screening of DR used by the doctors as a second aim for detection and identification the stages of this disease with more accurate and precise ways. DR is one of the most prevalent worldwide diseases that leading cause of blindness due to the damage blood vessels in the eye from elevated blood sugar (Salz and Witkin, 2015).

It can be treated if the diagnosis shows that patient with diabetes that holds early signs of retinopathy otherwise it will be ended with a complete loss of vision. The most common form of DR can be classified onto two stages; Non-proliferative and Proliferative (Skaggs *et al.*, 2017).

The main symptoms are usually observed in Non-PDR stage; microaneurysm dots, haemorrhages, cotton and wool spots, hard exudate, loops, venous bleeding, and Capillary leakage causes Diabetic Macular Edema (DME).

Early diagnosis in Non-proliferative can prevents vision loss in human beings. In contrast, Proliferative is the most advanced stage. It occurs

* **Corresponding Author:**
Bazhdar Noureddin Sheikh Mohammed
E-mail: bazhdar.sh.mohammed@su.edu.krd
Article History:
Received: 04/03/2019
Accepted: 03/09/2019
Published: 05/12 /2019

when the retina starts to grow abnormal blood vessels. This is called Neovascularization (NVE). The formation of these new vessels is easy fragile and either make few dark floaters if they bleed little and If they bleed a lot, blood diffuses through the vitreous chamber then might cause loss of visual capacity (Dodson, 2007). Figure 1, depicts a comparison between the symptoms in Non-PDR and PDR cases in DR.

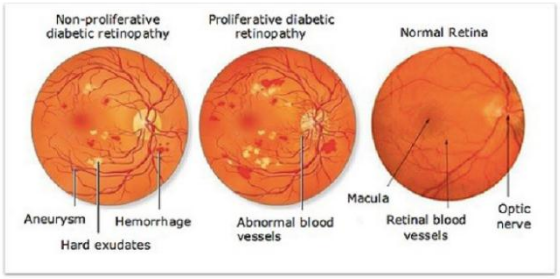

Figure1: The symptoms of Non-PDR and PDR.

Screening Programmed reduces the workload which usually the physicians faced and plays an important role in quality assurance tasks. Medical image analysis allows scientists and ophthalmologists to make a better decision about the stage of this disease. Many screening techniques in the last years have been devoted to detect automatically and classify stages DR, such as fundus photography, fluorescein angiography, B-scan ultrasonography and monochromatic photography (Salz and Witkin, 2015).This technology is called Computer Aided Diagnosis (CAD).

CAD provides useful information about the nature and status of the effect of diabetes on the eye (Verma *et al.*, 2011). Till now there has been no single modality software exist to satisfy all requirements for automatically screening. Recently many algorithms have been developed to diagnose image. Besides, increasing the number of patients, the detection methods have to be increased as well. The goodness of any screening method is determined by how accurate this technique to address the different stages of DR.

The main objective this work is presenting an artificial intelligence system to detect DR cases according to three classes: Normal, Non-PDR and PDR based on Neutrosophic set domain and statistical set domain that make the ophthalmologists and doctors give a better decision to the patients about the phases of the disease.

1. MATERIALS AND METHODS

In this work, 150 (1240x1488) fundus images divided into three different sets of Normal, Non-PDR, and PDR classes were used. 50 images are defined as Normal. 50 images are Non-PDR and last 50 images are PDR. The digital images have been collected from the DRIVE database project (Staal *et al.*, 2004).All the images have been accepted and reviewed by expert ophthalmologists. Figure 2, represents the flow chart diagram of the proposed method which splits mainly into two structures offline and real-time system.

First of all, in an offline method, the collecting data went through image pre-processing stage. The images from each category (Normal, Non-PDR, and PDR) were resized to (576x576) to reduce processing time. Secondly, all the images were changed from RGB to grayscale, to get uniform intensity before denoising them by the median filter. Then the images were enhanced with adaptive histogram equalization to increase their visual quality and contrast (Gonzalez and Woods, 2003).

After, the statistical and textural features from each fundus image were extracted in spatial and NS domain. In the spatial domain the gray level was by two techniques; GLCM, and GLRLM. From GLCM probabilistic distribution was generated to derive difference statistics features. From NS domain, the images were derived based upon True (T), Indeterminate (I), and False (F). Later all matrices were introduced to the stage of statistical features extraction and calculation at the output of this stage. The feature vector (Fv) was produced to easy describe important characteristics from images. Then, the all features were analyzed by using ANOVA1.

In ANOVA1 test, only those features are remained that make the images clinically significant. To test the powerful of suggested method the data were split onto training\testing sets. Finally, the performance measurements

used to evaluate the ability of the method and different image arguments. Besides, in a real-time system, the fundus photographs undergo the same pre-processing. During analyzing, significant features are selected from them and a feature three vector is formed for each image before introducing to the proposed classifiers to give a decision about each image individually either it belongs to Normal, Non-PDR, or PDR.

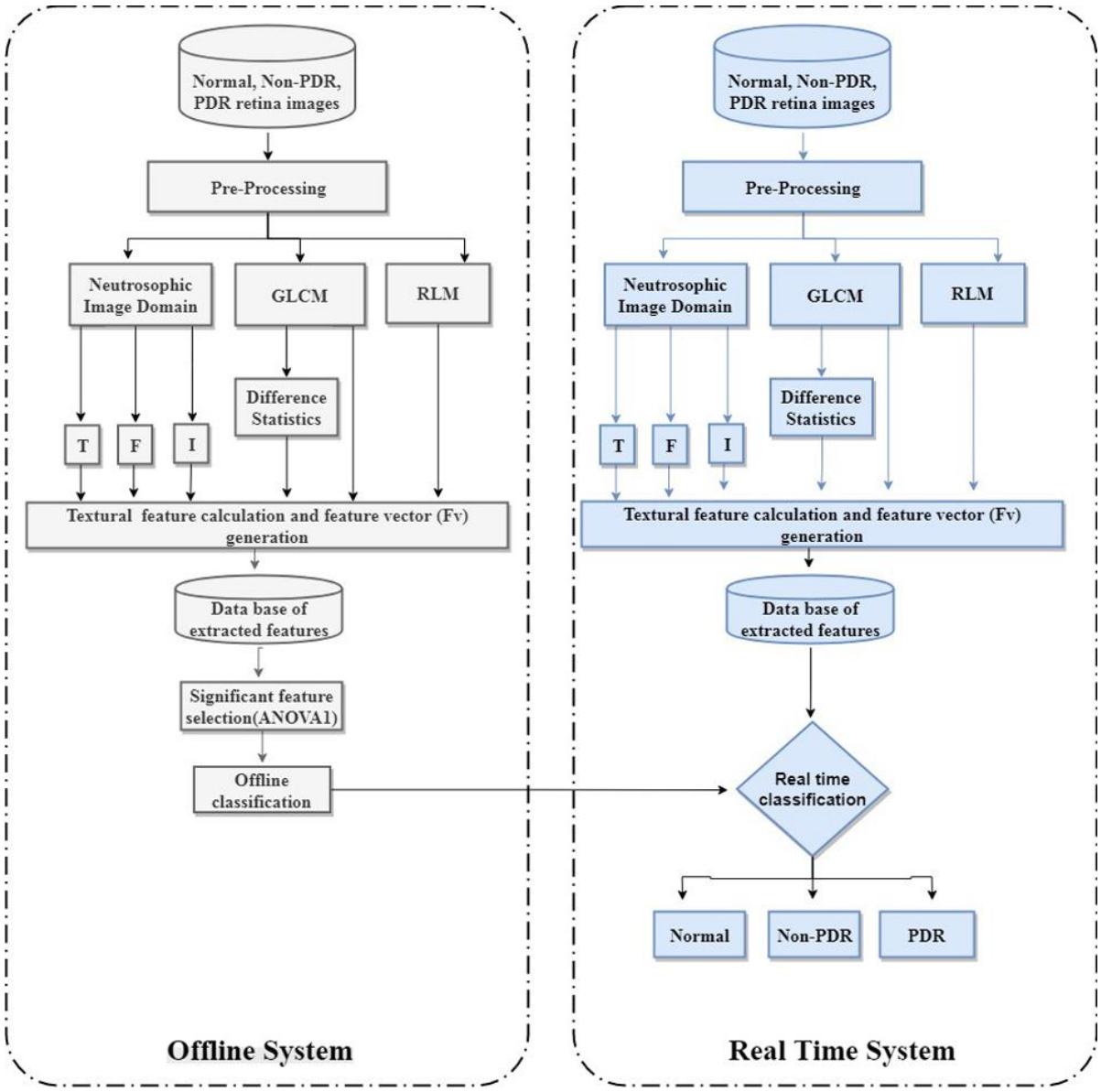

Figure 2: Block diagram of proposed method.

1.1 Extraction features

The main purpose of extracting features from the data is to increase the differentiate images, reduce the original data characteristics during the analysis process, and improves the accuracy of classification output (Ahmed, 2016, Yaba, 2016). The features from the data were extracted by performing: Neutrosophic and Statistical features.

1.1.1 Neutrosophic Image Feature Extraction

The Neutrosophic concept is a branch of philosophy was found by Smarandache and it has been employed widely in some branch of sciences especially founds impressively in image processing like medical image segmentation (Smarandache, 2005). A Neutrosophic set domain studies the origin, nature, and scope of neutralizing and their interactions with different ideational spectra. In NS,an image becomes more

suitable and uniform for the human viewer. The probability in NS image (PNS) can be represented in three components; T, I and F., which means that the pixel is T% true, I% indeterminate and F% false. T, I and F are functions undertaken by any known or unknown parameters. Each component has a value of [0, 1]. Figure. 3, Shows T.F, I and Homogeneity domain.

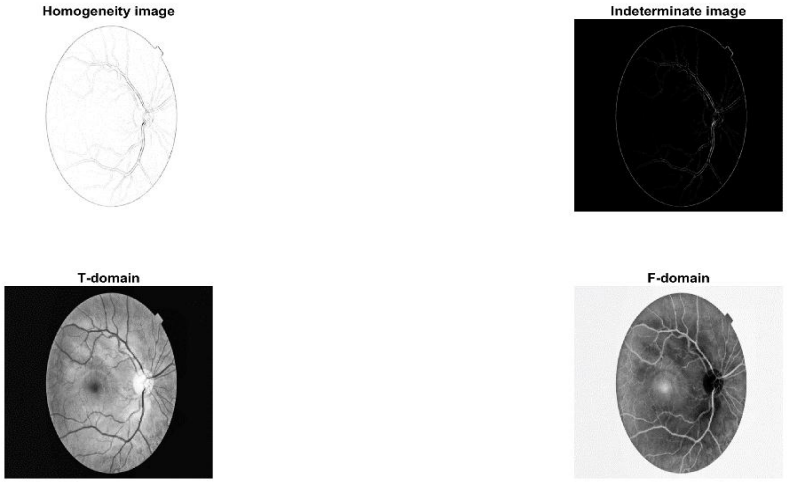

Figure 3: True, False, Indeterminacy, and Homogeneity components for DR image.

Any pixel P in image domain is defined as P(T,I,F) then pixel p(i,j) in image domain is transformed into the Neutrosophic set domain p(i,j)={T(i,j),I(i,j),F(i,j)}, where T(i,j),I(i,j) and F(i,j) are values for each membership. The intensity of the pixel (i,j) can be shown as g(i,j). Let U be a universe of discourse,and W is a set in U composed of light pixels. Each part of the transformation algorithm can be defined as (Salama *et al.*, 2017) (Eisa, 2014):

$$\overline{g(i,j)} = \frac{1}{wxw}\sum_{n=i-\frac{w}{2}}^{i+\frac{w}{2}} \sum_{n=j-\frac{w}{2}}^{j+\frac{w}{2}} g(m,n) \quad (1)$$

$$T(i,j) = \frac{\overline{g(i,j)}-\overline{g_{min}}}{g_{max}-g_{min}} \quad (2)$$

$$I(i,j) = \frac{\delta(i,j)-\delta_{min}}{\delta_{max}-\delta_{min}} \quad (3)$$

$$F(i,j) = 1 - t(i,j) \quad (4)$$

$$\delta(i,j) = |\ g(i,j) - \overline{g(i,j)}\ | \quad (5)$$

Where (g(i,j)) is the local mean value of the pixels of the window size in the level domain and δ(i,j) homogeneity value of T at (i,j). Homogeneity describes the local information, especially in segmented image. Neutrosophic images appeared by three matrices: object, edge, and background. In common probability white pixel values for object part, the probability of non-white pixel values for background membership, and for limit between a
non-white and white probability of the boundary was proposed. Neutrosophic set features for a particular component is described by three set of features; GLCM. RLM, and Difference statistics features and described each one according to T,F, and I components (Salama et al., 2017):

Entropy feature; it measures the disorder of an image. When the elements are not uniform to each other then they make of entropy increase.

$$En_{NS} = En_T + En_F + En_I \quad (6)$$

$$En_T = \sum_{i=1}^{N} \sum_{j=1}^{N} P_T(i,j) ln P_T(i,j) \quad (7)$$

$$En_F = \sum_{i=1}^{N} \sum_{j=1}^{N} P_F(i,j) ln P_F(i,j) \quad (8)$$

$$En_I = \sum_{i=1}^{N} \sum_{j=1}^{N} P_I(i,j) ln P_I(i,j) \quad (9)$$

Contrast feature; it measures the illuminance level between the pixels, or color that makes an object to be distinguished.

$$CO_{NS} = CO_T + CO_F + CO_I \quad (10)$$

$$CO_T = \sum_{i=1}^{N} \sum_{j=1}^{N} (i-j)^2 P_T(i,j) \quad (11)$$

$$CO_F = \sum_{i=1}^{N} \sum_{j=1}^{N} (i-j)^2 P_F(i,j) \quad (12)$$

$$CO_I = \sum_{i=1}^{N} \sum_{j=1}^{N} (i-j)^2 P_I(i,j) \quad (13)$$

Energy feature; it measures the quantity of elements which corresponds to the mean squared value of the signal.

$$En_{NS} = E_T + E_F + E_I \quad (14)$$

$$E_T = \sqrt{\sum_{i=1}^{N} \sum_{j=1}^{N} P_T(i,j)^2} \quad (15)$$

$$E_F = \sqrt{\sum_{i=1}^{N} \sum_{j=1}^{N} P_F(i,j)^2} \quad (16)$$

$$E_I = \sqrt{\sum_{i=1}^{N} \sum_{j=1}^{N} P_I(i,j)^2} \quad (17)$$

Homogeneity feature; it measures how much closes the surrounding distribution elements to the diagonal of the image matrix.

$$HO_{NS} = HO_T + HO_F + HO_I \quad (18)$$

$$HO_T = \sum_{i=1}^{N} \sum_{j=1}^{N} \frac{P_T(i,j)}{1+|i-j|} \quad (19)$$

$$HO_F = \sum_{i=1}^{N} \sum_{j=1}^{N} \frac{P_F(i,j)}{1+|i-j|} \quad (20)$$

$$HO_I = \sum_{i=1}^{N} \sum_{j=1}^{N} \frac{P_I(i,j)}{1+|i-j|} \quad (21)$$

1.1.2 Statistical Features

In an extraction features step, GLCM, GLRLM, and difference statistics were used for combinations the intensity of pixels value. GLCM used as two dimensional matrices of joint probabilities corresponding to the relative frequency of occurrence of pairs, with a distance d between them in a given direction (Alsmadi, 2017). Some of the statistical features were utilized in this paper are Homogeneity, Energy, Entropy Contrast, Symmetry, Correlation, and Momentum 1, Momentum 2, Momentum 3, Momentum 4, Angular 2nd Momentum Difference, Contrast Difference, Mean Difference, Entropy Difference, Short Run Emphasis, Long Run Emphasis, Run Percentage, Gray Level Non-Uniformity, and Run Length Nonuniformity.

Haralick developed a set of texture features from GLCM for an image to measure both first and second order statistics (Haralick *et al.*, 1973, Haralick, 1979). Gray level co-occurrence matrix (GLCM) for an image of size M x N is represented as(Acharya *et al.*, 2011):

$$C_d(i,j) = |\{(p,q),(p+\Delta x, q+\Delta y): I(p,q) = i, I(p+\Delta x, q+\Delta y) = j\}| \quad (22)$$

Where i, j defined as spatial coordinates, position operator $d = (\Delta x, \Delta y)$, the below equation used to find the grayscale probability of a pixel at $(\Delta x, \Delta y)$:

$$P_d(i,j) = \frac{C_d(i,j)}{\sum C_d(i,j)} \quad (23)$$

1.2 Classifiers

Neural Network is presumed as one of the most powerful technique that widely applied on many biomedical processes to recognizing types of disease and classify them to test a constructed models or diagnostic systems based on mathematical operations (Ismail and Yaba, 2015). To guess the output classes according to Normal, Non-PDR, and PDR, three classification methods were suggested: MUSVM, NB, and DF classifier.

1.2.1 Multi-Class support vector machine (MUSVM)

In general, SVM is a nonlinear learning algorithm with high generalization ability to classify images. It performs to classify problems of two groups of sets. SVM classifier determines the best hyperplane which distinguishes between each positive and negative training sample (Chamasemani and Singh, 2011). Multi-class classification problems usually are handled to categorize the features according to more than two binary categories (k >2). To solve MUSVM problems, normally the feature variables in a feature vector are proportional to the number of labels. In common two special approaches are available: one-versus-rest (Hong and Cho, 2008) and one-versus-one (Milgram *et al.*, 2006). These two strategies can split the multi-class problem to multiple binary classification subproblems for training data set. The output training set can be set up to carry out predictions about a test sample (Chamasemani and Singh, 2011).

1.2.2 Naïve Bayesian (NB)

The NB model is a heavily simple and effective method in machine learning. It can predict class labels form on a strong conditional independence assumption. Therefore, the probability of one feature does not make any effect on the other independence assumptions (Mukherjee and Sharma, 2012). The NB algorithm depends on the information of the comparable restricted pixels that already classified in training sets. Suppose C, are classes and m refers to possible classes $C = \{C_1, C_2, C_3, \dots, C_m\}$ for the domain of training set D in n-dimensional vector $D = \{D_1, D_2, D_3, \dots, D_n\}$. The classifier model estimates that $X \in D_i$ if and only if it has the maximum posteriori probability conditioned on D (Noronha *et al.*, 2014).

$$P(C_i|D) > P(C_j|D) \quad , \quad 1 \le j \le m, \quad j \ne i \quad (24)$$

By applying Bayes' rule to calculate the probability of a document D in a class C:

$$P(C_j|D) = \frac{P(D|C_j)P(C_j)}{P(D)} \quad (25)$$

Where P(D) has constant size for all classes, while only $P(D|C_j)P(C_j)$ required to be maximized.

2.1.1 Decision Forest (DF)

The random decision it is an attractive tree predictor tool for appraising image regression. It is decided by the distribution of trees separately and the correlation between them to operate datasets (Breiman, 2001). The main point of the tree is randomly select observations and specified features in a feature vector to produce multiple decision trees from the number of trees and then average the results. After that, the algorithm will select the class before are they restricted through bagging technique. Bagging algorithm is used to show de-correlation between training sets in order to decrease the variance of the model (James *et al.*, 2013).

1.3 Performance Measurements

To weigh the effectiveness of proposed method, the confusion matrix (error matrix) tool was employed as a statistical performance to evaluate the classification model(Stehman, 1997). The parameters such as Accuracy, Sensitivity, Specificity, Precision, and F1-Score are computed for each iteration (Trevethan, 2017):

$$\text{Sensitivity} = \frac{T_p}{T_p+F_N} * 100 \quad (26)$$

$$\text{Specificity} = \frac{T_N}{F_p+T_N} * 100 \quad (27)$$

$$\text{Accuracy} = \frac{T_p+T_N}{T_p+T_N+F_p+F_N} * 100 \quad (28)$$

$$\text{Precision} = \frac{T_p}{T_p+F_p} * 100 \quad (29)$$

$$\text{F1\_score} = \frac{2T_p}{2T_p+F_P+F_N} * 100 \quad (30)$$

Where, TP, TN, FP and FN represent True Positive, True Negative, False Positive, and False Negative, respectively. The train and test data sets were split into three-fold cross-validation as represented in Table 1.

Table 1. Splitting the input data into the training and testing sets.

Cross folds	Splitting ratio
1st training	30% Training 70% Testing
2nd training	70% Training 30% Testing
3rd training	30% Training (Random) 70% Testing

To predict the output classifier the input fields were specified into class labels. Classes with their corresponding labeled number are represented in Table 2. One-way analysis of variance (ANOVA1) was performed to select the succeeded features among all applying features (Hogg and Ledolter, 1987). It is usually a comparison method to indicate how close or far away from the means between the groups and within the groups. ANOVA decision represents the probability of occurrence (p-value) value. If the p-value is too small or near to zero, in this case, the null hypothesis is rejected and suggests that at least one sample means among all tested groups is significantly different as compared to the other samples mean (Acharya *et al.*, 2009).

Table 2. Class labels

Classes	Numbers
Normal	1
Non-PDR	2
PDR	3

2. RESULTS

Among 38 applied features after preb processing step, 16 features were selected by ANOVA1 with their p-values <0.001 to increase the accuracy of the method and to become more suitable to overcome the case of the disease. The succeeded features have been shown in Table 3.

Table 3. List of selected features according to their p-values.

Features Name	Feature Number	p-value
NS-Energy	2	3.7767815e-07
NS-Symmetry	5	2.7919764e-05
NS-Correlation	6	8.5578876e-13
NS-Moment 3	9	1.6331283e-05
NS-Short Run Emphasis	11	6.5423865e-07
NS-Run Percentage	13	8.5175199e-09
NS-Gray Level Non-Uniformity	14	0.00081359183
NS-Run Length Non-Uniformity	15	6.4482585e-08

NS-Angular Second Moment	16	4.3907629e-05
NS-Contrast Difference	17	1.2192163e-08
NS-Mean Difference	18	3.7640087e-08
NS-Entropy Difference	19	3.1124333e-07
Homogeneity	20	3.3957011e-06
Entropy	22	6.4770609e-14
Angular Second Moment	35	4.4096184e-05
Entropy	38	1.3581388e-17

Box graph usually is used to test and show relationships between categorical variables to provide more information about the samples. In Figure 4, two successive features are drawn which retrieved from Table 3, to show a difference between the groups means. From both, a clear separation seen that corresponds to statistically significant features to differentiate between the DR cases in clinical observation.

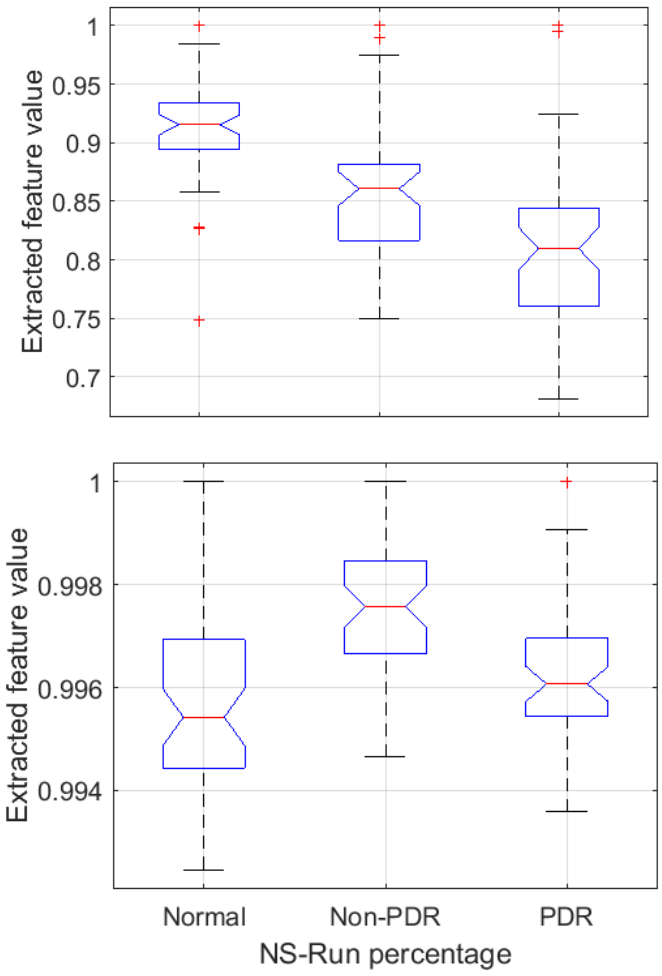

Figure 4: Box graph for two passed features: Entropy and NS-Run percentage.

Tables 4 and 5, illustrate four measurements; Accuracy (Acc), Sensitivity (Se), Specificity (Sp), and Precision (Pre) which found in a confusion matrix to show the best correctness results among final results of suggest method which were classified according to previously mentioned classification techniques. From Table 4, represents the outcome results when only the spatial domain was used to extract features, the ability of the system was poor to distinguish the differences between the stages due to the low percentage values of classification measurements. In contrast, in Table 5, there is a significant increase of performance classification has been seen after the features were extracted from both spatial and Neutrosophic domain which gives suitable output for clinical observation.

Table 4. Performance measurements for each classification method without NS features.

Classification Methods	Training Sets	Acc (%)	Sn (%)	Sp (%)	Pre (%)
MUSVM	1	75.2	91.4	67.1	58.1
	2	71.1	96.6	56.7	53.8
	3	47.6	100	21.4	38.8
Naïve Bayes	1	54.2	91.4	35.7	41.5
	2	68.9	86.7	60	52
	3	40.9	100	51.1	36
Decision forest	1	63.8	80	55.7	47,4
	2	77.8	80	76.6	63.1
	3	41.9	91.2	43.8	36.4

Table 5. Performance measurements for each classification method with NS features.

Classification Methods	Training Sets	Acc (%)	Sn (%)	Sp (%)	Pre (%)
MUSVM	1	93.3	88.6	95.7	91.1
	2	95.5	100	93.3	88.2
	3	93.3	94.3	92.8	86.8
Naïve Bayes	1	72.3	80	68.5	56
	2	86.6	93.3	83.3	73.8
	3	72.3	80	68.5	56
Decision forest	1	82.8	82.8	82.8	70.7
	2	93.3	93.3	93.3	87.5
	3	81.9	100	72.8	64.8

Figure 5, represents the comparison between the accuracy of the method with and without NS-domain. In MUSVM the accuracy raised to more than 95.5 %, while it was about 75% before applying NS. While, In NB classification, the final outcome changes about 70% and nearly 87% for both NS and without NS. Additionally, the accuracy increased by approximately 14% in DF and finally reached 93.3%.

The table of confusion matrix is drawn in Figure 6, describes the superior of the method due to the less inequality between actual and predicted data set classes. Among the all estimations less than %6 error occurred. In Contrast, best performance measurement achieved from MUSVM classifier for diagnosis the preferred stages in diabetic retinopathy with average accuracy about 95.5%.

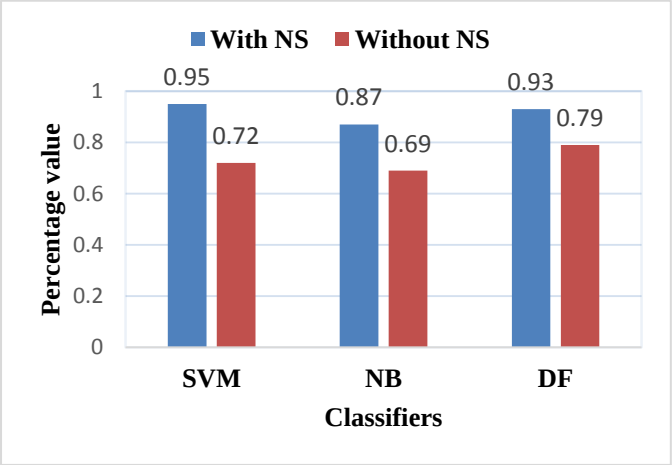

Figure 5. Accuracy improvement by NS-domain.

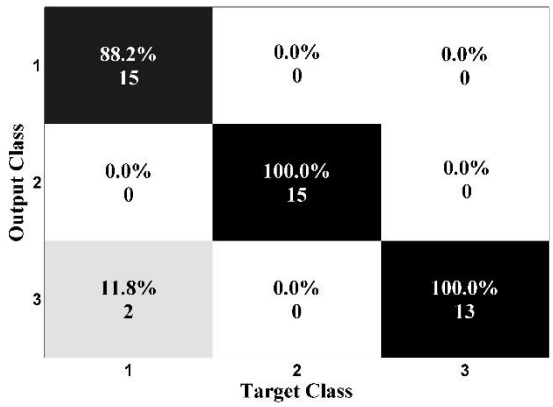

Figure 6: Confusion matrix table.

3. DISCUSSION

Many authors suggested different methods to automatically classify the DR stages. Nayak et al., applied two texture features; Area of blood vessels and exudate area on 140 fundus images contain Normal, Non-PDR, and PDR cases to extract the main different characteristics between the images. The data was classified by ANN classifier (Nayak *et al.*, 2008).To analyze the abnormal signs from early stage of DR with normal stage , Reza et al., extracted hard exudate, cotton and wool spots, and large plaque of hard exudate from 60 images and classify them according to Normal, Mild, Moderate, and severe stages. To find the information gain within the method, Decision support system was used (Reza and Eswaran, 2011). Five texture features were extracted from 238 fundus images that divided onto Normal, Non-PDR, PDR, and macular edema. In this work, the features were fed into SVM classifier to evaluate the performance the model (Acharya *et al.*, 2012). Nornoha et al., used fundus retinal images to classify 272 fundus images according to normal, mild glaucoma and sever glaucoma by using feature-based machine learning classification approach. For this aim, 3rd order cumulant features was used. Then, the images fed into 10-fold cross validation technique and tested by SVM classifier (Noronha et al., 2014). In another work has been done by Mane et al., hybrid features named holo-entropy features applied on 130 fundus images to

extract retinal blood vessel area and optic disk region on a set of images which contain Normal and DR images. Finally, the images were classified by using decision tree classification technique (Mane and Jadhav, 2017). An automated classification method approached by Islam et al., to classify 180 fundus images according to normal and PDR. In this approach, bag of words model with Speeded Up Robust Features utilizes; 87 images contain microaneurysms, haemorrhages hard exudates, and soft exudates. For a classification purpose, the data split into %65 and %35 training-testing sets. The performance achieved by SVM classifier (Islam *et al.*, 2017).Table 6, represents a list contains a performance measurement comparison between some recently related works and our approached method for automatically diagnosis DR.

4. CONCLUSIONS

Diabetic retinopathy is a global disease of vision loss. It happens in the retina in the back of the eye due to the complication of diabetes inside blood vessels. It ends with blindness if left untreated. Screening is a key part of the diagnosis of early stages of that disease. In this

paper a new way offered to automatically classify fundus images according to Normal, Non-PDR, and PDR groups. The standard images are available in DRIVE project database. The images were extracted using statistical and textural features based on neutrosophic set domain. About thirty-eight features in both domains were applied on images to generate a feature vector. Among them, only sixteen succeeded features selected by ANOVA1 which are viable in medical practice. The collected features were undergone MUSVM, NB, and DF classification models after the data was split into training and testing sets by using three-fold cross validation technique. After analyzing the dataset, the results in MUSVM classifier represented that the suggested method able to classify the DR images with best performance measurement: accuracy 95.5%, sensitivity 100%, and specificity 93.3%. So, the system can be used as a second tool by ophthalmologists to check DR.

Conflict of Interest

There is no conflict of interest.

Table 6. Comparison between related works.

Author (Year)	No. of images	Features	Performance	Acc (%)	Sn (%)	Sp (%)	Detection
(Nayak et al., 2008)	140	Texture	ANN	93	90	100	Normal, Non-PDR, and PDR
(Reza and Eswaran, 2011)	60	Hard and soft exudate area	Decision support system	97.2	100	97	Non-PDR
(Acharya et al., 2012)	238	Texture Analysis	SVM	-	98.9	89.5	Normal, Non-PDR, PDR, and Edema
(Noronha et al., 2014)	272	Higher order statistics	NB	92.6	100	92	Normal, mild, and moderate\severe
(Mane and Jadhav, 2017)	130	Hybrid holo-entropy, and wavelet	DF	97	96.7	96.4	Normal and abnormal
Islam et al., (2017)	180	Speeded Up Robust Features	SVM	94.4	94.8	94	Normal and DR
Our proposed method	150	Neutrosophic and Statistical	MUSVM	95.5	100	93.3	Normal, Non-PDR, and PDR

References

ACHARYA, U. R., LIM, C. M., NG, E. Y. K., CHEE, C. & TAMURA, T. 2009. Computer-based detection of diabetes retinopathy stages using digital fundus images. *Proceedings of the institution of mechanical engineers, part H: journal of engineering in medicine,* 223**,** 545-553.

ACHARYA, U. R., NG, E. Y.-K., TAN, J.-H., SREE, S. V. & NG, K.-H. 2012. An integrated index for the identification of diabetic retinopathy stages using texture parameters. *Journal of medical systems,* 36**,** 2011-2020.

AHMED, R. M. 2016. Using Logistic Regression to Distinguish Between Fatty and Fibroid Masses in Medical Imaging (Ultrasound Image). *ZANCO Journal of Pure and Applied Sciences,* 28**,** 193-201.

ALSMADI, M. K. 2017. An efficient similarity measure for content based image retrieval using memetic

algorithm. *Egyptian journal of basic and applied sciences*, 4**,** 112-122.

BREIMAN, L. 2001. Random Forests. *Machine Learning*, 45**,** 5-32.

CHAMASEMANI, F. F. & SINGH, Y. P. 2011. Multi-class support vector machine (SVM) classifiers--an application in hypothyroid detection and classification. Bio-Inspired Computing: Theories and Applications (BIC-TA), 2011 Sixth International Conference on,. IEEE, 351-356.

DODSON, P. M. 2007. Diabetic retinopathy: treatment and prevention. *Diabetes and Vascular Disease Research*, 4**,** S9-S11.

EISA, M. 2014. A new approach for enhancing image retrieval using neutrosophic sets. *International Journal of Computer Applications*, 95.

GONZALEZ, R. & WOODS, R. 2003. Digital Image Processing 2nd ed: Pearson Education.

HARALICK, R. M. 1979. Statistical and structural approaches to texture. *Proceedings of the IEEE*, 67**,** 786-804.

HARALICK, R. M., SHANMUGAM, K. & DINSTEIN, I. H. 1973. Textural features for image classification. *IEEE Transactions on systems, man, and cybernetics*, 3**,** 610-621.

HOGG, R. & LEDOLTER, J. 1987. Engineer statistics. *England: MacMillan Publishing Company*.

HONG, J.-H. & CHO, S.-B. 2008. A probabilistic multi-class strategy of one-vs.-rest support vector machines for cancer classification. *Neurocomputing*, 71**,** 3275-3281.

ISLAM, M., DINH, A. V. & WAHID, K. A. 2017. Automated diabetic retinopathy detection using bag of words approach. *Journal of Biomedical Science and Engineering*, 10**,** 86.

ISMAIL, H. J. & YABA, S. P. 2015. Enhanced Accuracy and Reliability of ER and PR Immunohistochemistry Scoring Using ANN from Digital Microscope Images. *ZANCO Journal of Pure and Applied Sciences*, 27**,** 69-80.

JAMES, G., WITTEN, D., HASTIE, T. & TIBSHIRANI, R. 2013. *An introduction to statistical learning*, Springer.

MANE, V. M. & JADHAV, D. V. 2017. Holoentropy enabled-decision tree for automatic classification of diabetic retinopathy using retinal fundus images. *Biomedical Engineering/Biomedizinische Technik*, 62**,** 321-332.

MILGRAM, J., CHERIET, M. & SABOURIN, R. "One against one" or "one against all": Which one is better for handwriting recognition with SVMs? tenth international workshop on Frontiers in handwriting recognition, 2006. SuviSoft.

MUKHERJEE, S. & SHARMA, N. 2012. Intrusion detection using naive Bayes classifier with feature reduction. *Procedia Technology*, 4**,** 119-128.

NAYAK, J., BHAT, P. S., ACHARYA, R., LIM, C. M. & KAGATHI, M. 2008. Automated identification of diabetic retinopathy stages using digital fundus images. *Journal of medical systems*, 32**,** 107-115.

NORONHA, K. P., ACHARYA, U. R., NAYAK, K. P., MARTIS, R. J. & BHANDARY, S. V. 2014. Automated classification of glaucoma stages using higher order cumulant features. *Biomedical Signal Processing and Control*, 10**,** 174-183.

REZA, A. W. & ESWARAN, C. 2011. A decision support system for automatic screening of non-proliferative diabetic retinopathy. *Journal of medical systems*, 35**,** 17-24.

SALAMA, A., EISA, M. & FAWZY, A. 2017. A Neutrosophic Image Retrieval Classifier. *International Journal of Computer Applications*, 170**,** 975-8887.

SALZ, D. A. & WITKIN, A. J. 2015. Imaging in diabetic retinopathy. *Middle East African journal of ophthalmology*, 22**,** 145.

SKAGGS, J. B., ZHANG, X., OLSON, D. J., GARG, S. & DAVIS, R. M. 2017. Screening for Diabetic Retinopathy Strategies for Improving Patient Follow-up. *North Carolina medical journal*, 78**,** 121-123.

SMARANDACHE, F. 2005. *A Unifying Field in Logics: Neutrosophic Logic. Neutrosophy, Neutrosophic Set, Neutrosophic Probability: Neutrsophic Logic. Neutrosophy, Neutrosophic Set, Neutrosophic Probability*, Infinite Study.

STAAL, J., ABRAMOFF, M. D., NIEMEIJER, M., VIERGEVER, M. A. & VAN GINNEKEN, B. 2004. Ridge-based vessel segmentation in color images of the retina. *IEEE Trans Med Imaging*, 23**,** 501-9.

STEHMAN, S. V. 1997. Selecting and interpreting measures of thematic classification accuracy. *Remote sensing of Environment*, 62**,** 77-89.

TREVETHAN, R. 2017. Sensitivity, specificity, and predictive values: foundations, pliabilities, and pitfalls in research and practice. *Frontiers in public health*, 5**,** 307.

VERMA, K., DEEP, P. & RAMAKRISHNAN, A. 2011. Detection and classification of diabetic retinopathy using retinal images. India Conference (INDICON), 2011 Annual IEEE, IEEE, 1-6.

YABA, S. P. 2016. Breast cancer detection system based oncomprehensive wavelet features of mammogram images and neural network. *ZANCO Journal of Pure and Applied Sciences*, 27**,** 47-58.